Relationships between lightning flash rates and radar reflectivity vertical structures in thunderstorms over the tropics and subtropics

Chuntao Liu,[1] Daniel J. Cecil,[2] Edward J. Zipser,[1] Kevin Kronfeld,[3] and Roy Robertson[3]

[1] Relationships between the vertical profile of radar reflectivity and lightning flash rates are investigated using 13 years of Tropical Rainfall Measuring Mission (TRMM) observations during 1998–2010. First the Radar Precipitation Features (RPFs) are defined by grouping raining areas detected by the TRMM Precipitation Radar (PR). Then the characteristics of radar reflectivity and lightning flash rate are calculated in each RPF using PR and Lightning Imaging Sensor (LIS) observations. Using these RPFs, temperatures at 20, 30, and 40 dBZ radar echo tops, used as proxies of the maximum convective intensity of precipitation systems, are examined as indicators of the probability of lightning. Although 30 and 40 dBZ echo top temperatures are better indicators of the probability of lightning than the 20 dBZ echo top temperature, there is a large regional variation in the temperature thresholds, especially between land and ocean. In general, oceanic thunderstorms have higher 20 dBZ echo top and larger horizontal extent than those over land. However, radar reflectivity is more likely to exceed 30 and 40 dBZ at cold temperatures over land than over ocean. The correlations between flash rates and radar echo top temperatures, areas and volumes of radar reflectivity, and ice water contents in the mixed phase region are analyzed using RPFs with at least one flash. In agreement with previous studies, the correlations with the echo top temperatures are low, but the correlations between flash rates and areas and volumes of high radar reflectivity in the mixed phase region are much higher. There is a high correlation between the flash rates and the volumes with radar reflectivity greater than 30, 35, or 40 dBZ in the mixed phase region, but the correlation coefficient varies significantly between thunderstorms over different regions, especially between land and ocean. These results are confirmed by repeating the analysis for regions of the storms defined as convective, thus eliminating the contribution from large areas of stratiform radar echo that have much less lightning.

1. Introduction

[2] More than half a century ago, scientists had already attempted to understand the relationship between the lightning rate and the vertical structure of radar reflectivity in thunderstorms by using the lightning reports of surface observers and the first generation of weather radar [*Workman and Reynolds*, 1949; *Atlas*, 1958; *Shackford*, 1960].

[3] Good correlations between the radar reflectivity at altitudes and the lightning flash rate may be interpreted by the noninductive charging theory that collisions among radar sensitive precipitation ice particles and smaller cloud ice particles may separate the electric charge when supercooled liquid water is present. Owing to different terminal velocities, the ice particles carrying opposite charges could accumulate in different part of the storm and lead to strong electric fields and lightning. On the basis of laboratory studies, the noninductive charging mechanism is more efficient when precipitation size ice particles and supercooled liquid water coexist between about $-10°C$ and $-20°C$ [*Takahashi*, 1978; *Saunders and Peck*, 1998]. The noninductive charging as the dominant source of the lightning initiation is supported by the strong correlations between the amount of precipitation ice and the lightning flash rate using ground-based radar reflectivity and lightning observations in field campaigns [*Williams et al.*, 1989; *MacGorman and Rust*, 1999; *Petersen and Rutledge*, 2001; *Deierling et al.*, 2008]. Strong correlations with lightning were also found for updraft volume (10 and 20 m/s) and graupel volume in observations [*Wiens et al.*,

[1]Department of Atmospheric Sciences, University of Utah, Salt Lake City, Utah, USA.
[2]Earth System Science Center, University of Alabama in Huntsville, Huntsville, Alabama, USA.
[3]Rockwell Collins, Cedar Rapids, Iowa, USA.

2005; *Deierling and Petersen*, 2008] and simulations [*Fierro et al.*, 2006].

[4] Owing to complex microphysical processes in the storms that can vary with different convective intensities and environments, the efficiency of the noninductive charging mechanism in storms could be correspondingly different. This is evidenced by the lack of lightning over ocean that is well documented in the literature [e.g., *Wang*, 1963; *Orville and Henderson*, 1986; *Goodman and Christian*, 1993; *Zipser and Lutz*, 1994; *Boccippio et al.*, 2000; *Cecil et al.*, 2005]. However, size distributions of precipitation ice particles and supercooled liquid water are very difficult to measure in storms, compared to the radar reflectivity. Therefore different ways of relating the radar reflectivity vertical structure to the lightning flash rates have been studied, such as echo top height [*Williams*, 1985; *Ushio et al.*, 2001], maximum radar reflectivity at different altitudes [*Zipser and Lutz*, 1994; *Cecil and Zipser*, 2002; *Cecil et al.*, 2005; *Pessi and Businger*, 2009], and amount of ice retrieved from radar reflectivity [*Carey and Rutledge*, 2000; *Petersen et al.*, 2005; *Deierling et al.*, 2008]. These studies are either from some field campaigns with limited cases [e.g., *Carey and Rutledge*, 2000; *Deierling and Petersen*, 2008; *Deierling et al.*, 2008], or focused over certain regions [e.g., *Pessi and Businger*, 2009; *Mosier et al.*, 2011; *Xu et al.*, 2010], or limited to just a specific property derived from radar [e.g., *Petersen et al.*, 2005]. There has been no study systemically comparing the correlations between lightning rate and various properties of radar reflectivity in the storms over different regions with a global coverage, mainly due to the absence of sufficient observations.

[5] Since its launch in 1997, the Tropical Rainfall Measuring Mission (TRMM) [*Kummerow et al.*, 1998] satellite has been observing the various precipitation systems over the tropics and subtropics for more than 13 years. The precipitation radar (PR) on board TRMM has resolutions about 4 km in horizontal and 0.25 km in vertical and uniform calibration. The detailed vertical structures of the radar reflectivity by PR and the flash rates observed by the Lightning Imaging Sensor (LIS) are proven very valuable in studying the lightning and the structure of the thunderstorms [*Petersen et al.*, 2005; *Cecil et al.*, 2005; *Pessi and Businger*, 2009; *Xu et al.*, 2010]. The motivation of this study is to derive relationships between the lightning rate and the various radar reflectivity properties in the storms over different regions of the tropical and subtropical land and ocean. The questions to be addressed include the following:

[6] 1. How well can we use the vertical structure of radar reflectivity to quantitatively determine the probability of lightning and its regional variations?

[7] 2. What are the correlations between flash rate and radar reflectivity at different temperatures in the mixed phase region? What are the regional variations in these correlations, especially between thunderstorms over land and over ocean?

[8] 3. How accurately can we estimate thunderstorm flash rate by using the profiles of radar reflectivity and the retrieved ice water content?

[9] 4. What are the median characteristics of thunderstorms seen by precipitation radar and how do they vary regionally? What is the minimum radar reflectivity as a function of height or temperature for a thunderstorm and its regional variations?

[10] To answer these questions, 13 years of TRMM PR and LIS observations during 1998–2010 have been collocated. Then the Radar Precipitation Features (RPFs) are defined by grouping the areas with rain retrieved by the PR. The properties of radar reflectivity from the PR and lightning flash rate from LIS are determined for each RPF. With millions of RPFs and their radar and lightning properties, first, the probability of the lightning as function of the properties of radar reflectivity is discussed in section 3. Then the correlations between the properties of radar reflectivity and the lightning flash rates in RPFs are examined in section 4, with specific attention to regional differences. The conclusions are given in section 5.

2. Data and Methodology

[11] The primary tool used in this study is the precipitation feature database developed in the University of Utah [*Liu et al.*, 2008]. In this database, first the TRMM PR and LIS observations are collocated. Then the contiguous pixels in a TRMM orbit with nonzero near surface rainfall from TRMM 2A25 algorithm (PR-based rainfall retrieval algorithm) [*Iguchi et al.*, 2000] are grouped together and defined as Radar Precipitation Features (RPFs). The characteristics of radar reflectivity and the number of lightning flashes from LIS inside these RPFs are summarized (details in the work of *Liu et al.* [2008]). The flash rate in each RPF is estimated by dividing the number of flashes by the LIS view time (usually around 90 s). To limit noise, only RPFs with at least four contiguous PR pixels (with size $> \sim 80$ km^2) are used in this study.

[12] Because the noninductive charging process is temperature sensitive, and the PR only provides the observations as a function of altitude, it is important to convert the height dependence of radar reflectivity into temperature dependence. First, the temperature profile for each RPF is estimated by temporal and spatial interpolation of NCEP reanalysis data [*Kistler et al.*, 2001]. Then using these temperature profiles, properties describing the radar reflectivity vertical structures at temperature levels are derived. The temperatures from NCEP reanalysis should generally be lower than those encountered inside an updraft core, but we have no reliable way to characterize the true temperatures inside the RPF.

[13] The parameters to describe the radar reflectivity for each RPF include (1) temperatures at the altitude of maximum 20, 30, and 40 dBZ echo tops; (2) maximum radar reflectivity profile at particular temperature levels; (3) area having at least 20, 25, 30, 35, 40, and 45 dBZ at temperature levels from $-60°$C to $20°$C at $4°$C intervals; (4) volume having at least 20, 25, 30, 35, 40, and 45 dBZ between $-35°$C and $-5°$C; (5) Ice Water Contents (IWCs) retrieved within each volume having at least 20, 25, 30, 35, 40, and 45 dBZ from $-5°$C upward to the 20 dBZ echo top and from $-5°$C to $-35°$C

[14] Note that IWCs are estimated using the Z-M$_{ice}$ relationship derived from ground-based radar observations of storms over the Tiwi islands near Darwin Australia [*Carey and Rutledge*, 2000]. This relationship may not be accurate for storms over different regions. These parameters are used here only to give a common reference as the volumes of the storm but with more weight to higher

Table 1. Population of All Precipitation Features Defined by TRMM 2A25 Rain Area and Those With Lightning Flashes During 1998–2010[a]

	Open Oceans	Land	Coastal	All
All precipitation features	11.8 million	3.7 million	6.4 million	22 million
With flashes (thunderstorms)	59,421	426,754	171,660	657,835
Percentage with flashes	0.5%	11.5%	2.66%	3%
Flash rate > 10 flash/minute	3305	66957	19831	90063
Percentage with Flash rate > 10 flash/minute	0.03%	1.8%	0.31%	0.41%

[a]Here coastal region is the area within 1000 km of coastline of major continents. Open ocean is the area at least 1000 km away from coastline of major continents. The coastal region is shown with dotted lines in Figure 1.

reflectivity, likely to signify larger precipitation ice particles, for regional comparisons.

[15] A three-step approach is used to describe the correlations between the radar reflectivity properties and the flash rates in the RPFs. The first step is to determine the probability of the RPFs having at least one flash based on their maximum convective intensity indicated by the temperature of 20, 30, and 40 dBZ echo tops. Because the LIS views a particular point for 80–100 s, the minimum detectable flash rate for an RPF is about 0.6–0.8 flash per minute [*Cecil et al.*, 2005]. Therefore the results of this first step can only be used to infer the probability of a lightning rate greater than about one flash per minute at overpass time only, not for discriminating if a storm has lightning at any other time during its lifetime. After identifying the RPFs with lightning, the second step is to summarize the characteristics of radar reflectivity in the thunderstorms (RPFs with at least one flash at overpass time). The next step is to correlate the lightning flash rate to the various properties of radar reflectivity. Note that we cannot account for lagged relationships or effects of storm lifecycle, with TRMM providing a snapshot of flash rate and reflectivity. Besides showing the bulk correlations between the vertical profiles (and areas) of radar reflectivity and the flash rates in thunderstorms over land, ocean, and coastal regions (defined as over ocean but within 1000 km of a continent), the regional variations of these correlations are analyzed by using RPFs in each $4° \times 4°$ box between 36°S and 36°N.

[16] Because the stratiform region of the RPFs could have a large volume of ice but contribute a small proportion of the charge separation due to the weak updrafts and less super-cooled liquid water, it is important to repeat these steps but using only the convective regions of the RPFs. Therefore the Convective Region features (CRF) are defined by grouping the areas with convective precipitation from TRMM 2A23 algorithm [*Awaka et al.*, 1998]. The set of parameters describing the radar reflectivity at temperature levels similar to those of RPFs are derived for each CRF. The lightning flash rate in each CRF is calculated using the number of flashes within CRFs. The similar three-step analysis is repeated for CRFs to validate the results of RPFs.

3. Probability of Lightning as a Function of Radar Reflectivity Structure

[17] A total of 22 million RPFs are identified over 36°S–36°N from 13 years of TRMM PR observations from 1998 to 2010. Only 3% of them have at least one flash (Table 1). More RPFs have flashes over land (11%) than those over open oceans (0.5%). This is consistent with the results of many earlier studies [e.g., *Vorpahl et al.*, 1970; *Orville and*

Henderson, 1986; *Zipser and Lutz*, 1994; *Williams and Stanfill*, 2002; *Toracinta et al.*, 2002; *Christian et al.*, 2003; *Cecil et al.*, 2005]. Over the coastal region, there is a higher ratio (2.66%) of the RPFs with flashes than those over open oceans. This land versus ocean contrast is clearly shown in Figures 1b and 1c. The detailed regional differences of thunderstorm population are also shown by percent of RPFs with lightning flashes over both land and ocean. For example, there is relatively higher percentage (around 20%) of RPFs with flashes over Sahel, central and South Africa, Argentina, northern India and Pakistan, United States, and Mexico than other regions over land (Figure 1c). A larger proportion of RPFs off the coast of major continents and over subtropical oceans, such as the South Pacific Convergence Zone (SPCZ), have more flashes than those in the Inter-tropical Convergence Zone (ITCZ) over equatorial oceans (Figure 1c). About 1.8% of the RPFs over land have more than 10 flashes per minute (Table 1), more over Sahel, central Africa, southeast United States, Argentina, India and Pakistan (Figures 1d and 1e). Intense oceanic RPFs with more than 10 flashes per minute are mostly found close to continents, over subtropical oceans, including the SPCZ, and north Atlantic and Pacific (Figures 1d and 1e). Here, 0.3% of RPFs within 1000 km of a coastline have 10 flashes per minute, which is about 10 times more frequent than those in open oceans (Table 1). All these results are consistent with the precipitation feature analysis using microwave radiometer observations [*Liu et al.*, 2011].

3.1. Probability of Lightning Versus Maximum Convective Intensity

[18] To present the probability of lightning in RPFs as the function of their convective intensity, all RPFs over land, open ocean, and coastal regions are binned by their 20, 30, and 40 dBZ echo top temperatures. Then the probability of the lightning in each bin is estimated by the percentage of the RPFs with at least one lightning flash. The results are shown in Figure 2. It is clear that both the 30 dBZ and especially the 40 dBZ echo top temperatures are very good indicators of the probability of lightning in RPFs over land, ocean, and coastal regions. This is consistent with many earlier studies [e.g., *Shackford*, 1960; *Marshall and Radhakant*, 1978; *Williams and Geotis*, 1989; *Rutledge et al.*, 1990; *Rutledge and Petersen*, 1994; *Lang et al.*, 2000]. In comparison 20 dBZ echo top temperature is almost irrelevant to the probability of lightning. This strongly suggests that lightning initiation is related to high radar reflectivity reaching high altitudes and cold temperatures but not to low radar reflectivity. Because radar reflectivity is very sensitive to the hydrometeor particle
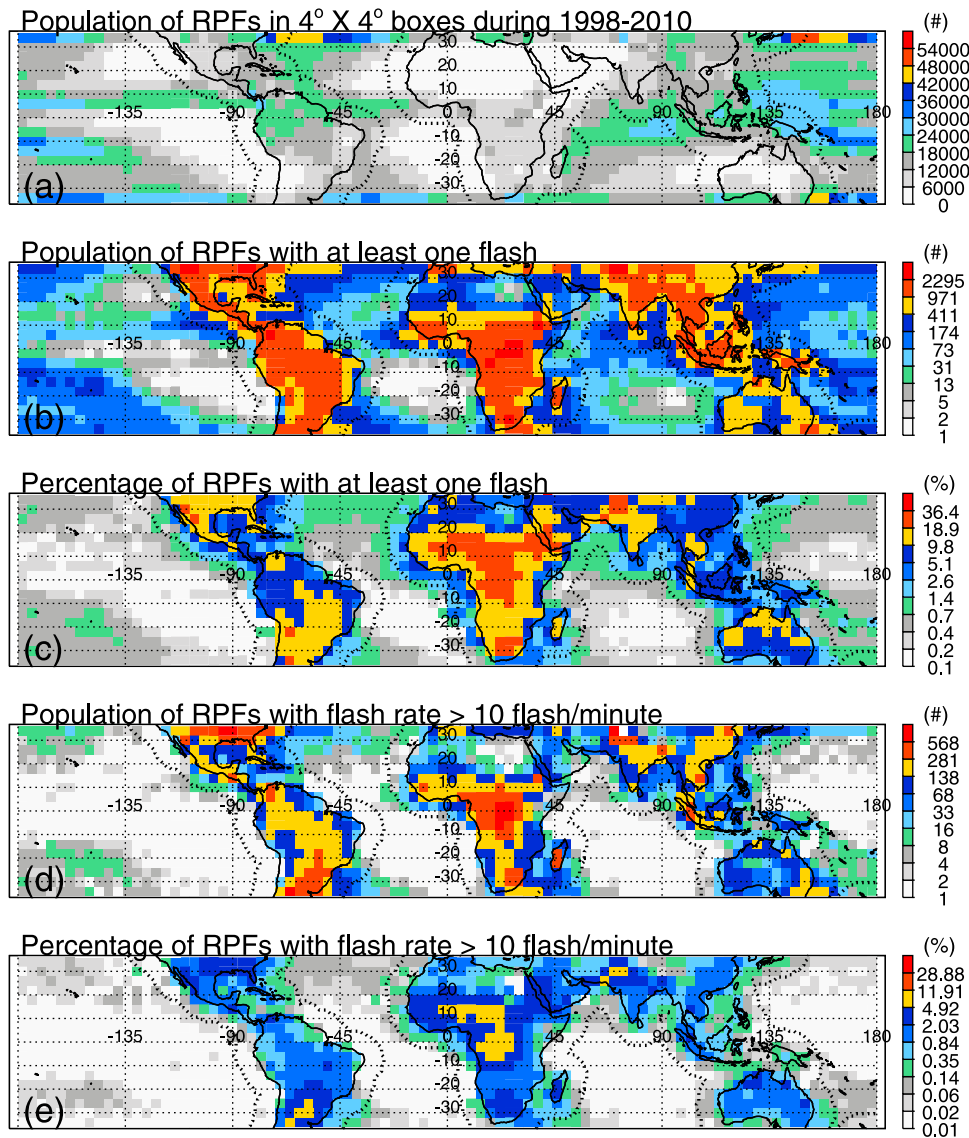
Figure 1. (a) Population of precipitation features defined by rain area from TRMM TMI 2A25 product (RPFs) in $4° \times 4°$ boxes during 1998–2010. (b) Population of RPFs with at least one flash. (c) Percentages of RPFs with at least one flash in $4° \times 4°$ boxes. (d) Population of RPFs with flash rate >10 flash per minute. (e) Percentage of RPFs with flash rate >10 flash per minute. Note that there are more samples near 30°S and 30°N by TRMM, therefore Figures 1a, 1b, and 1d are biased to high values at the subtropical regions. The sample bias is removed with the fraction calculation in Figures 1c and 1e.

sizes, this tends to confirm the consensus in the literature that the presence of large ice particles at cold temperatures is very important in charge separation and lightning initiation. Deep convection with weak updrafts could lift small ice particles and have 20 dBZ echo top reaching very cold temperatures, but without large ice particles, the lightning probability in these systems is still low.

[19] Note that there are some cases with very cold 20 dBZ echo top temperature (<−40°C) but warm 30 dBZ echo top (>0°C) with high percentage of lightning over land (Figures 2a and 2e). Most of those cases are observed at the edge of the PR swath and may be explained by the RPFs missing convective cores that are just outside the PR swath.

[20] Confirming some earlier studies [*Toracinta et al.*, 2002; *Cecil et al.*, 2005; *Liu et al.*, 2010], for a given 30 dBZ echo

top temperature, RPFs over land are more likely to have lightning than those over the coastal regions and open ocean (Figures 2a, 2c, and 2e and Figures 3a and 3b). This also means that for the same probability of lightning, oceanic RPFs have colder echo top temperatures than RPFs over land (Table 2) [*Petersen et al.*, 1996; *Vincent et al.*, 2003]. The 30 dBZ echo top temperatures corresponding to a 50–50 chance of lightning are −38.7°C for ocean and −20.1°C for land. There is less difference for 40 dBZ echo tops, −11.5°C for ocean and −6.0°C for land. Values from coastal regions are a little closer to the values from land regions. To have a marginal (10%) probability of lightning, RPFs over land have to have 30 dBZ/40 dBZ echo top temperature below −9.5°C/4.1°C, in contrast to −13.5°C/−1.5°C for those over coastal regions and −19°C/−4.6°C for those over open oceans.
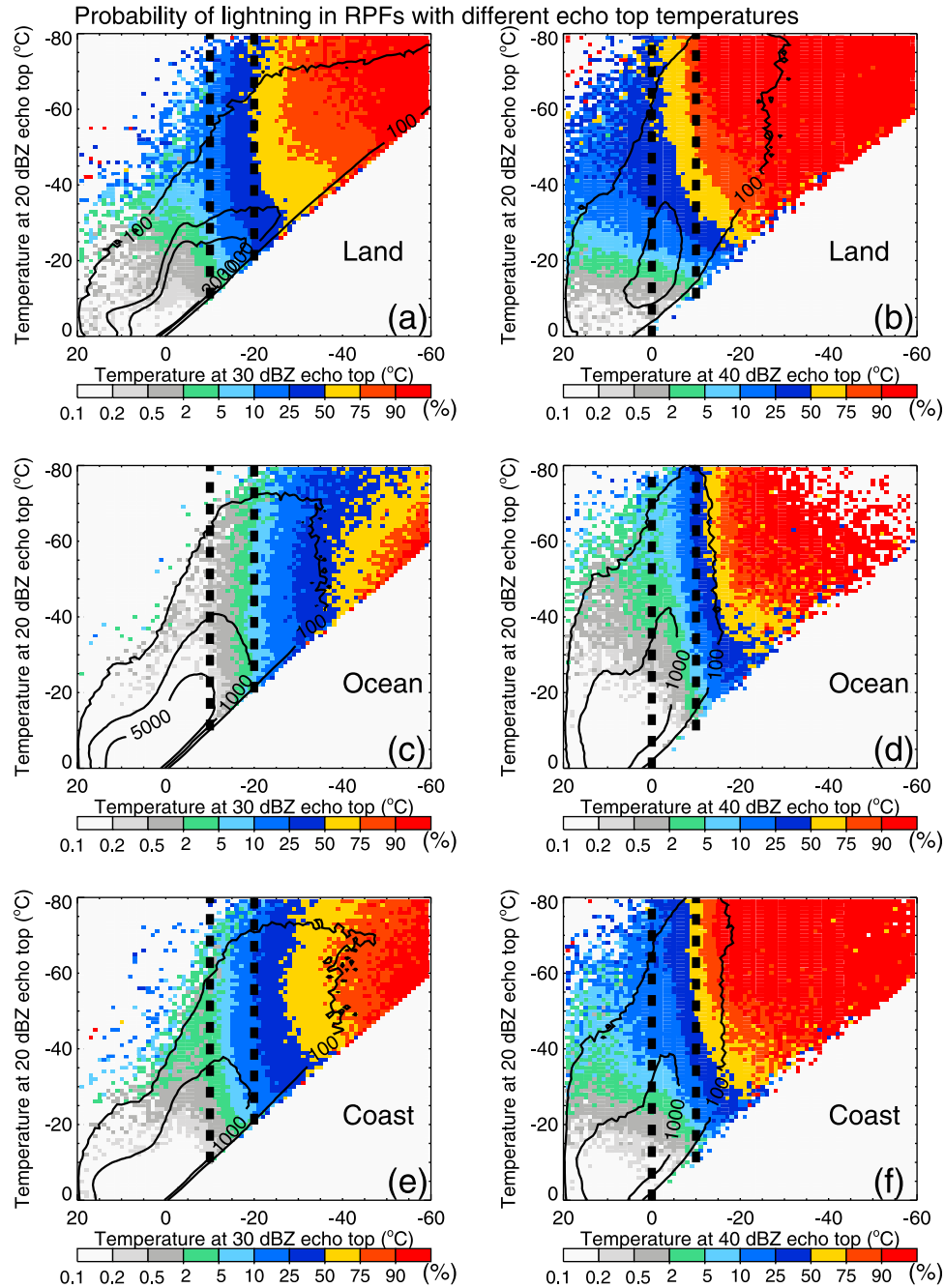
Figure 2. Probability of lightning in RPFs as the function of the echo top temperatures. (a) Probability of lightning as the function of 20 and 30 dBZ echo top temperatures in the RPFs over land. (b) Probability of lightning as the function of 20 and 40 dBZ echo top temperatures in the RPFs over land. (c) Same as Figure 2a but for the RPFs over ocean. (d) Same as Figure 2b but for the RPFs over ocean. (e) Same as Figure 2a but for the RPFs over coastal region. (f) Same as Figure 2b but for the RPFs over coastal region. Note the log color scale for values below 10% and linear color scale for values above 10%.

[21] In addition to the obvious land versus ocean differences, there are some regional variations of the probability of lightning for the RPFs with the same radar reflectivity properties. For example, for RPFs over tropical oceans, Figure 3a shows an especially low probability of lightning over the central Pacific, compared with the east Pacific close to Central America or the east Atlantic close to Africa, or the northern Indian Ocean. The sense of these differences is similar whether the 30 dBZ echo top is −10°C or −20°C. For RPFs over land, with 30 dBZ echo top temperature near −10°C, the probability of lightning is relatively high over Sahel, South Africa, Northern Australia, and Northern India (Figure 3a). These are all locations well known for strong and frequent thunderstorms, so this result is not unexpected. However, comparing Figures 3a with 3 d, using −20°C instead of −10°C for the 30 dBZ echo top, and a color table
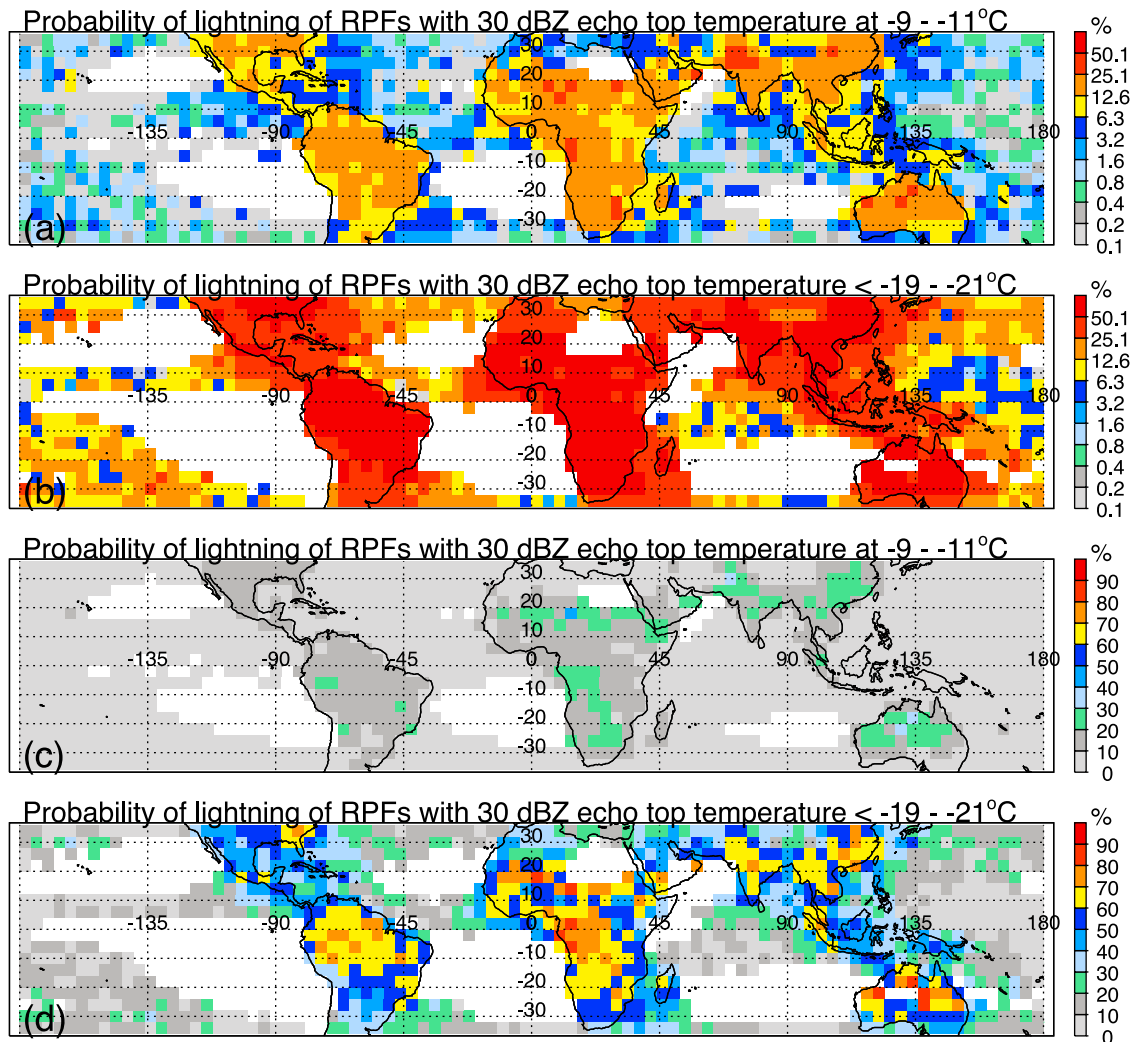
Figure 3. (a) Percentage of RPFs with 30 dBZ echo top temperature around −10°C with at least one lightning flash in 4° × 4° boxes. (b) Same as Figure 3a except around −20°C. (c and d) Same as Figures 3a and 3b but with different color scales to better distinguish higher probabilities. Results only show for 4° × 4° boxes with at least 20 samples.

that distinguishes the higher lightning probabilities better, the regional differences are not the same. For the same threshold of −20°C, the southeastern United States has a higher lightning probability than the southwestern United States, and the Amazon has a higher probability than Argentina. The reason for these differences will be explored later but may well require additional research.

[22] Figure 4 shows regional differences but for the two thresholds used for 40 dBZ, 0°C and −10°C. For oceans, it is obvious that the low occurrence of 40 dBZ echoes reaching cold temperatures in most tropical locations except close to continents hampers regional comparisons, especially in the deep tropics far from continental influences. Over land, it is interesting to note that lightning is also more likely to occur over mountain regions, such as southwest United States, Tibet, and Andes (Figures 4a and 4c). In Figure 4d, given a 40 dBZ echo top reaching −10°C, there is a high probability of lightning over the Amazon, land and ocean close to Central America, much of Africa, and most of Asia and over land and ocean from India and China through Indonesia

and northern Australia, with much lower probabilities over subtropical oceans.

### 3.2. Characteristics of Radar Reflectivity in RPFs With Flash

[23] Figure 5 compares the frequency distributions of area exceeding 20, 30, or 40 dBZ at different temperature levels in thunderstorms. First, the area with at least 20 dBZ in oceanic thunderstorms tends to be larger than those over land at temperature levels warmer than −50°C in general (Figure 5a). However, a much smaller proportion of oceanic thunderstorms have 30 or 40 dBZ echo at cold temperatures. The area with at least 30 dBZ in oceanic thunderstorms is larger than over land at temperature levels warmer than −20°C but smaller than in land thunderstorms at levels colder than −20°C, the main differences applying to the more extreme cases (Figure 5b). The area with at least 40 dBZ in oceanic thunderstorms is larger than in their land counterparts at levels warmer than −10°C but is also smaller at colder temperatures, also for the more extreme cases

Table 2. The 30 and 40 Echo Top Temperatures of RPFs With the Probability of LIS Lightning at About 10, 20, 50, and 75%

Echo Top Temperature (°C)	Ocean	Land	Coastal	All
30 dBZ echo top T with 10% lightning	−19.0	−9.5	−13.5	−12.5
30 dBZ echo top T with 20% lightning	−24.2	−12.4	−16.9	−16.0
30 dBZ echo top T with 50% lightning	−38.7	−20.1	−25.7	−25.1
30 dBZ echo top T with 75% lightning	−55.3	−29.2	−37.0	−36.5
40 dBZ echo top T with 10% lightning	−4.6	4.1	−1.5	−1.1
40 dBZ echo top T with 20% lightning	−6.9	−0.9	−3.8	−3.6
40 dBZ echo top T with 50% lightning	−11.5	−6.0	−8.2	−8.0
40 dBZ echo top T with 75% lightning	−17.6	−10.4	−12.2	−12.1

(Figure 5c). The thunderstorms over the coastal regions have the properties in between those over land and over ocean (not shown).

[24] In general, oceanic precipitation systems have weaker updrafts and cannot lift large precipitation ice particles to high altitudes [e.g., *Lucas et al.*, 1994; *Zipser and Lutz*, 1994]. However, the smaller ice particles in these systems can still reach near the tropopause. Land systems have stronger updrafts and may lift large ice particles up to much colder temperature levels with higher super cooled liquid water content. The weaker updrafts may lead to the lower super cooled liquid water content in the oceanic systems [*Stith et al.*, 2004]. This has been shown with the land versus ocean contrast in convective systems by comparing radar and infrared observations [*Liu et al.*, 2007]. In general oceanic thunderstorms have larger areas covered by specific reflectivity values than those over land. Small precipitation ice particles in oceanic thunderstorms may produce large areas of 20 dBZ echo at all heights and temperatures (Figure 5a). However, without strong updrafts, large precipitation ice
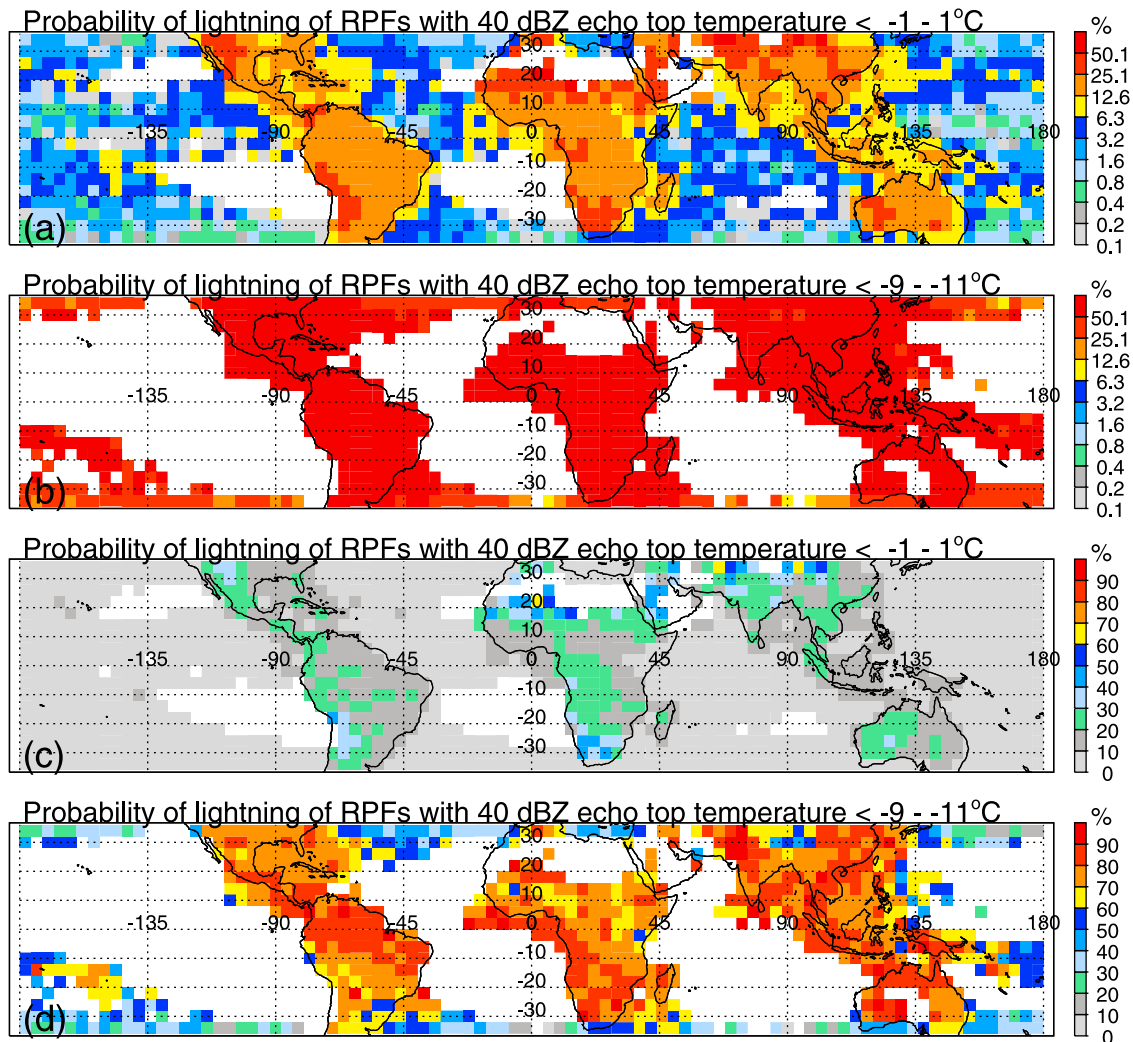
Figure 4. (a) Percentage of RPFs with 40 dBZ echo top temperature around 0°C with at least one lightning flash in 4° × 4° boxes. (b) Same as Figure 4a except around −10°C. (c and d) Same as Figures 4a and 4b but with different color scales to better distinguish smaller probabilities. Results only show for 4° × 4° boxes with at least 20 samples.
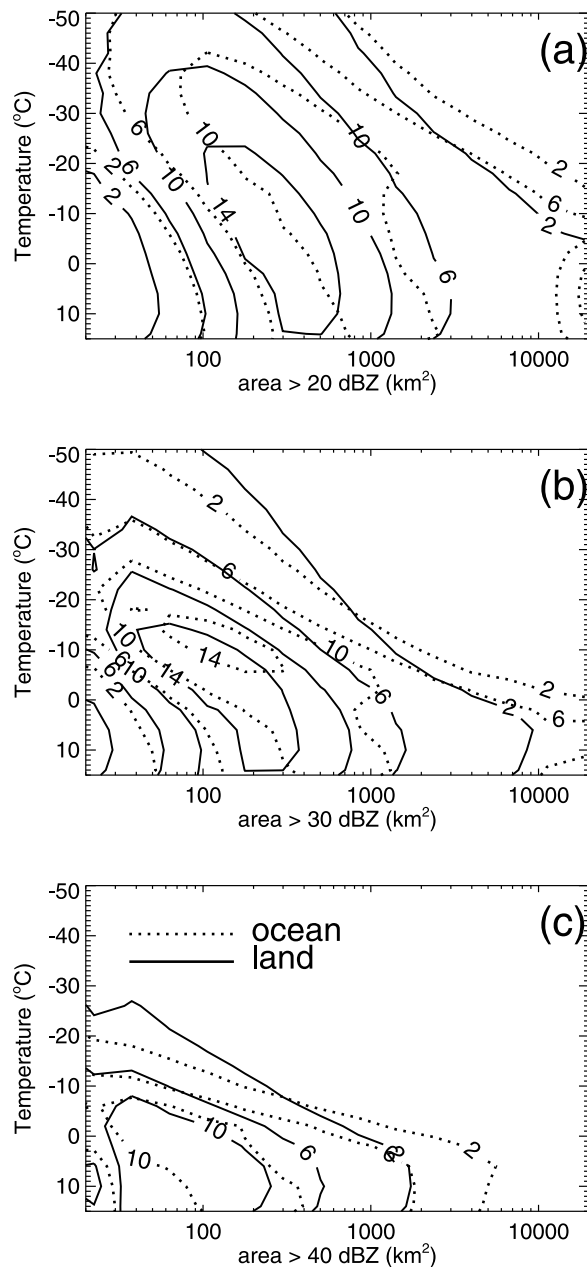
Figure 5. (a) Frequency distribution of the areas with PR reflectivity greater than 20 dBZ at different temperature levels within thunder RPFs over land (solid) and ocean, with units in percent. (b) Same as Figure 5a except for areas with reflectivity greater than 30 dBZ. (c) Same as Figure 5a except for areas with reflectivity greater than 40 dBZ.

particles cannot be lifted to colder temperature levels and produce areas of 30 and 40 dBZ in these oceanic thunderstorms as large as those sometimes observed over land (Figures 5b and 5c).

4. Correlation Between the Properties of Radar Reflectivity and the Flash Rate

[25] In this section, a set of parameters describing the radar reflectivity is used to test their correlations with the flash rates in RPFs that do have flashes. Radar echo top

temperatures and maximum radar reflectivities represent the maximum convective intensity of thunderstorms. Area and volume of radar reflectivity greater than certain values represent the size and number of the convective core(s) and the area or volume occupied by large ice particles. Ice water content derived from radar reflectivity is basically another measure of volume-integrated radar reflectivity but is weighted more heavily by higher radar reflectivity values. Examples of the scatterplots of the flash rate and a few selected properties of RPFs with flashes are shown in Figure 6. Echo top temperature shows only a weak relationship with flash rate (Figure 6a), but the area containing at least moderate reflectivity at the $-10°C$ level shows a much stronger linear relationship (Figure 6b). Adding a level of complexity to compute the echo volume (Figure 6c) or IWC (Figure 6d) only slightly tightens the relationship, compared to simply using echo area (Figure 6b).

4.1. Radar Echo Top Temperature and Maximum Radar Reflectivity

[26] The correlation coefficients between flash rate and the 20, 30, and 40 dBZ echo top temperature in the RPFs with flashes over land, ocean, and coastal regions are listed in Table 3. The correlations between flash rate and echo top temperatures (and heights) are very low (Table 3 and Figure 6a). Only 40 dBZ echo top temperatures have correlations as high as 0.5 with the flash rate. This suggests that there are large variations in the relationship between echo top and the flash rate for different thunderstorms, and using a specific dBZ echo top to estimate flash rate could lead to a large error for individual thunderstorms.

[27] Flash rates also do not have a good correlation with the maximum radar reflectivities at different levels in thunderstorms. As shown in Figure 7, the correlations are below 0.5 at all altitudes. The highest correlations about 0.4 are from flash rate to the maximum radar reflectivities near 7–8 km (with higher correlations for land than ocean). This tends to be around the $-10°C$ to $-20°C$ temperature range, somewhat consistent with the efficient charge separation at these temperatures with the noninductive charging mechanism.

[28] The low correlation coefficients from flash rate to the echo top and maximum radar reflectivity imply that the flash rate in thunderstorms is not as well correlated with the maximum convective intensity as it is with measures related to volume of at least moderate updrafts, such as volume of higher values of reflectivity in the mixed phase region. This is consistent with the earlier studies [*Wiens et al.*, 2005; *Fierro et al.*, 2006; *Deierling and Petersen*, 2008].

4.2. Area and Volume of Radar Reflectivity and Ice Water Content

[29] *Deierling and Petersen* [2008] have pointed out that the flash rate in thunderstorms is well correlated with the volume of updraft in the convective cores. TRMM cannot observe updrafts, and its horizontal resolution cannot adequately characterize the size of convective cores. But metrics based on the area and volume with high reflectivity at particular altitudes can account for differences in the number of strong convective cores in different RPFs. An RPF could contain a single convective core or a long line with several individual cores, all producing lightning. Because the noninductive charging mechanism is more efficient with
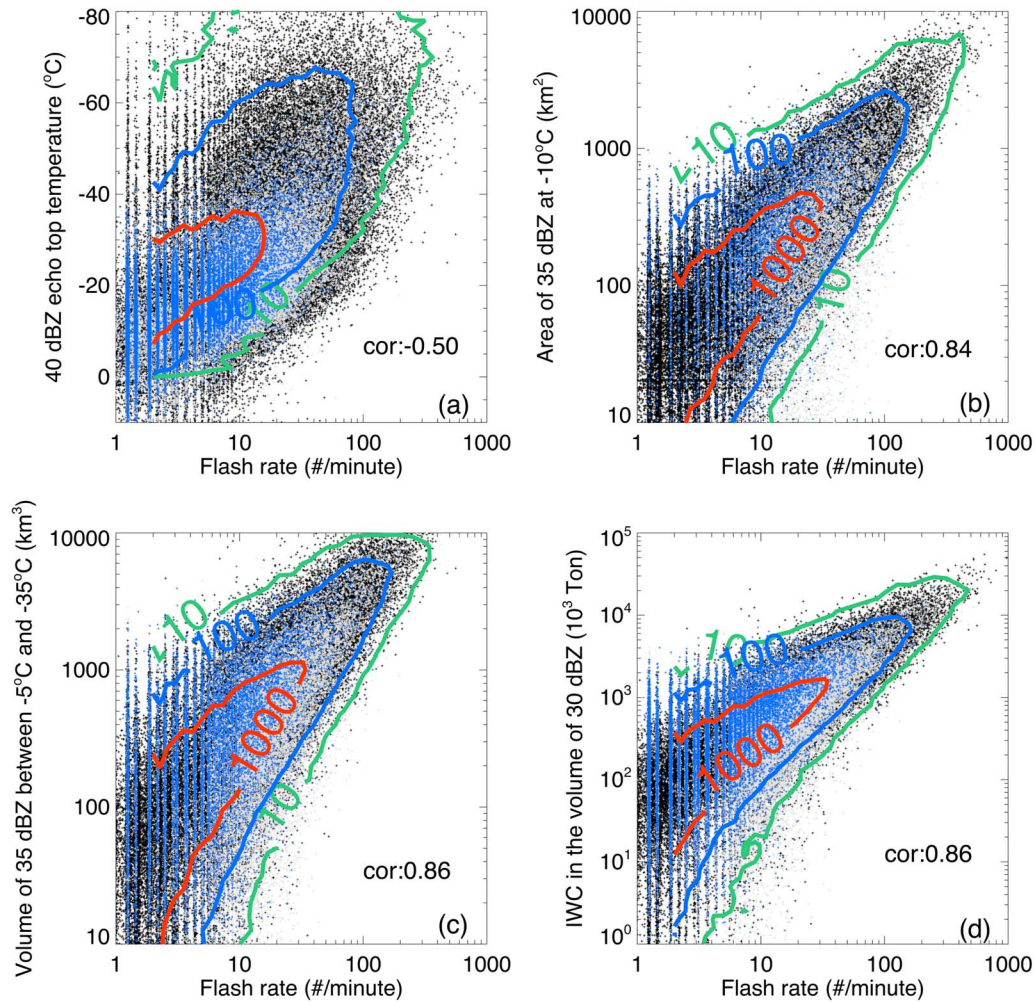
Figure 6. Scatterplot of RPFs over land (black dots), ocean (blue dots), and coastal regions (white dots) by their (a) 20 dBZ echo top temperature and flash rate, (b) area of 35 dBZ at −10°C and flash rate, (c) volume of 35 dBZ between −5°C and −35°C and flash rate, and (d) total ice water content in the volume of 30 dBZ from −5°C to echo top and flash rate. The contours show the 2-D histogram of population of RPFs over all regions.

Table 3. Correlation Coefficients Between Storm Flash Rate and Some Parameters Derived From PR Observations Within RPFs With Flashes in 36°S–36°N

	Ocean	Land	Coast	All 36°S–36°N
20 dBZ echo top temperature	−0.12	−0.27	−0.18	−0.24
30 dBZ echo top temperature	−0.30	−0.40	−0.36	−0.38
40 dBZ echo top temperature	−0.49	−0.49	−0.51	−0.50
Volume of 20 dBZ between −5°C and −35°C	0.35	0.58	0.46	0.49
Volume of 25 dBZ between −5°C and −35°C	0.50	0.76	0.64	0.68
Volume of 30 dBZ between −5°C and −35°C	0.65	0.85	0.82	0.82
Volume of 35 dBZ between −5°C and −35°C	0.76	0.86	0.86	0.86
Volume of 40 dBZ between −5°C and −35°C	0.81	0.83	0.85	0.83
Volume of 45 dBZ between −5°C and −35°C	0.77	0.75	0.79	0.76
IWC inside volume of 20 dBZ from −5°C to top	0.51	0.81	0.71	0.75
IWC inside volume of 25 dBZ from −5°C to top	0.66	0.86	0.82	0.83
IWC inside volume of 30 dBZ from −5°C to top	0.76	0.86	0.86	0.86
IWC inside volume of 35 dBZ from −5°C to top	0.82	0.84	0.86	0.84
IWC inside volume of 40 dBZ from −5°C to top	0.82	0.79	0.83	0.80
IWC inside volume of 45 dBZ from −5°C to top	0.76	0.72	0.76	0.72
IWC inside volume of 20 dBZ from −5°C to −35°C	0.49	0.80	0.68	0.72
IWC inside volume of 25 dBZ from −5°C to −35°C	0.64	0.85	0.80	0.82
IWC inside volume of 30 dBZ from −5°C to −35°C	0.75	0.86	0.85	0.86
IWC inside volume of 35 dBZ from −5°C to −35°C	0.80	0.85	0.86	0.85
IWC inside volume of 40 dBZ from −5°C to −35°C	0.81	0.81	0.84	0.82
IWC inside volume of 45 dBZ from −5°C to −35°C	0.76	0.74	0.77	0.74

supercooled liquid water, the focus is on the temperature levels between −5°C to −35°C. The correlations between flash rate and the volumes with reflectivities exceeding thresholds from 20 to 45 dBZ between −5°C and −35°C in thunderstorms over land, ocean, and coastal regions are listed in Table 3. The flash rate has high correlations (>0.76) with the volumes with reflectivity values greater than 35 dBZ for thunderstorms over both land and ocean (also see Figure 6c). However, the correlation with the volume of echo exceeding 20 dBZ is below 0.6. This implies that volumes with high radar reflectivity in the mixed phased region are more important than the volume with low reflectivity for lightning production. In other words, the presence of large particles is more important, as radar reflectivity is very sensitive to particle size. Note that correlations between flash rate and volumes of 20–35 dBZ in thunderstorms over land are higher than those over ocean. But the correlation to volumes with 40 dBZ is slightly higher in thunderstorms over coastal regions (0.85 versus 0.83).

[30] For oceanic cases, the correlations between flash rate and IWC are greater than those between flash rate and echo volume, probably because IWC gives added weight to the high reflectivity values that are somewhat rare aloft in oceanic convection. Computing IWC does not improve the correlations compared to using echo volume exceeding 30 dBZ (or higher thresholds) for land or coastal cases. In those groupings, a large volume of 30+ dBZ usually includes some reflectivities that are much greater, and there is likely a stronger correlation between the echo volume and IWC for the land and coastal groupings than the ocean grouping. The highest correlations with flash rate are from the IWC computed inside the volume of 30+ dBZ echo, as weaker reflectivities have little relevance to lightning.

[31] The correlation coefficients between the flash rate and the area exceeding different reflectivity thresholds at different temperature levels (Figure 8) are calculated for RPFs with flashes over land and ocean between 36°S and 36°N. For example, the area exceeding 35 dBZ at −10°C has a 0.70 correlation with flash rate for ocean and 0.86 correlation with flash rate for land. Without dividing into these groups, there is a 0.84 correlation with flash rate (see scatterplot in Figure 6b). The highest correlations with flash rate in thunderstorms over land are from the area satisfying reflectivity thresholds around 30 dBZ at −30°C to 45 dBZ at −5°C (Figure 8a). For oceanic thunderstorms, the highest correlations with flash rates are with the areas exceeding thresholds around 35 dBZ at −30°C to 45 dBZ at −10°C (Figure 8a). The highest value of correlation is 0.86 for 40 dBZ at −6°C over land and 0.83 for 40 dBZ at −10°C over ocean. We suggest that the high correlation with area exceeding 20–25 dBZ from −30°C to −40°C over land is not due to active charge separation at those cold temperatures but because these conditions are often accompanied by much higher reflectivity in mixed phase regions in thunderstorms over land. However, over ocean, the cases with 20–25 dBZ reaching −40°C more rarely have 30 dBZ echoes reaching −10°C due to the weaker updrafts in oceanic convection. Therefore the correlation between flash rate and area exceeding 20–25 dBZ at temperatures colder than −30°C are quite low in oceanic thunderstorms (Figure 8a).

[32] One could argue that the area of the RPF often includes a broad stratiform region that contributes little to the total RPF flash rate. Figure 8b accounts for this by repeating the analysis for convective regions only. The results are essentially the same as in Figure 8a, except the low correlations from weak reflectivity thresholds and warm temperatures go away. This is not surprising since the area satisfying 30+ dBZ well above the freezing level is almost exclusively from convective regions anyway.

[33] The areas exceeding different reflectivity thresholds as a function of temperature in Figure 8 obviously have high correlations with each other. To account for this and identify which combinations of reflectivity and temperature are most relevant to flash rate, Figure 9 removes the partial correlation coefficients. For a given reflectivity (Z)- temperature (T) combination, we subtract the linearly predicted flash rate from the observed flash rate for each RPF. Then the correlation coefficients as in Figure 8 are recreated using the residual of the flash rate. If these resulting correlation coefficients are high, then the combination Z and T had little independent influence on the flash rate. These correlation coefficients are averaged over the entire reflectivity-temperature domain and assigned to the value (Z, T). The
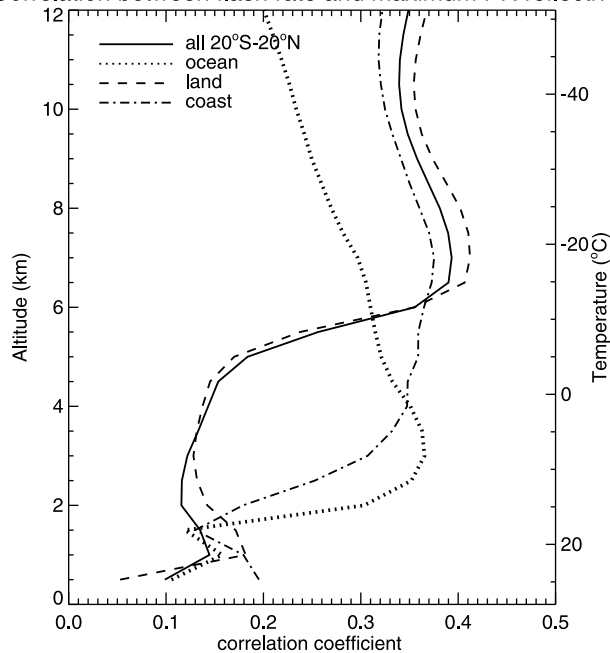
Figure 7. Correlation coefficient between flash rate and the maximum radar reflectivity at different heights in RPFs with flashes over land and ocean in 20°S–20°N. The climatology of the temperatures of the altitude levels is shown. Note that the correlation coefficients are very low for cases in subtropics as well (not shown here).

process is repeated for all possible values of Z and T to produce Figure 9. The lowest values in Figure 9 indicate the (Z, T) combinations with the greatest control on flash rate.

[34] One of the most important features shown in Figure 9a is the importance of 30–40 dBZ between −10°C and −30°C

in the correlation to flash rate with low values (<0.1) of mean residual correlation. In particular, the strongest independent correlations are for area exceeding 30 dBZ near −20°C over land and 36 dBZ near −12°C over ocean. This is consistent with the temperature range of high charge separation of the noninductive charging theory [*Takahashi*, 1978; *Saunders and Peck*, 1998]. Repeating the same analysis for convective regions only, similar results are obtained (Figure 9b). There are some differences in the location of the highest correlations (lowest residual correlations; Figure 9a and b) between land and ocean that remain to be explored.

4.3. Regional Variation of the Relationship of Flash Rates to Radar Structure

[35] To investigate the regional variation of the correlations from the flash rate to the properties of radar reflectivity in thunderstorms, the correlation coefficients between flash rate and the parameters describing the radar reflectivity are calculated for RPFs with flashes in each 4° × 4° box. Some selected results are shown in Figure 10. Consistent with Table 3, the correlations from flash rates to 20 dBZ echo top temperatures (Figure 10a) and volume of 20+ dBZ echo (Figure 10b) are low globally. Higher correlations are found to the areas and volumes with high radar reflectivity values, such as area of 35 dBZ at −10°C and volume of 35 dBZ (Figures 10c and 10d). The correlation coefficients over land are greater than those over ocean, as in Table 3. Especially high correlations are found over Central and South Africa and Australia and to the IWC in the volume of 30 dBZ (Figure 10f). Correlations are low for the Maritime Continent, which might be expected with a mix of oceanic and land convection. Some of the correlations are also a bit lower for West Africa than for most other places known for vigorous convection. Of places known to have vigorous convection and high flash rates, the lowest correlations (around 0.7 in Figures 10c and 10d) are in Pakistan and northwestern India,
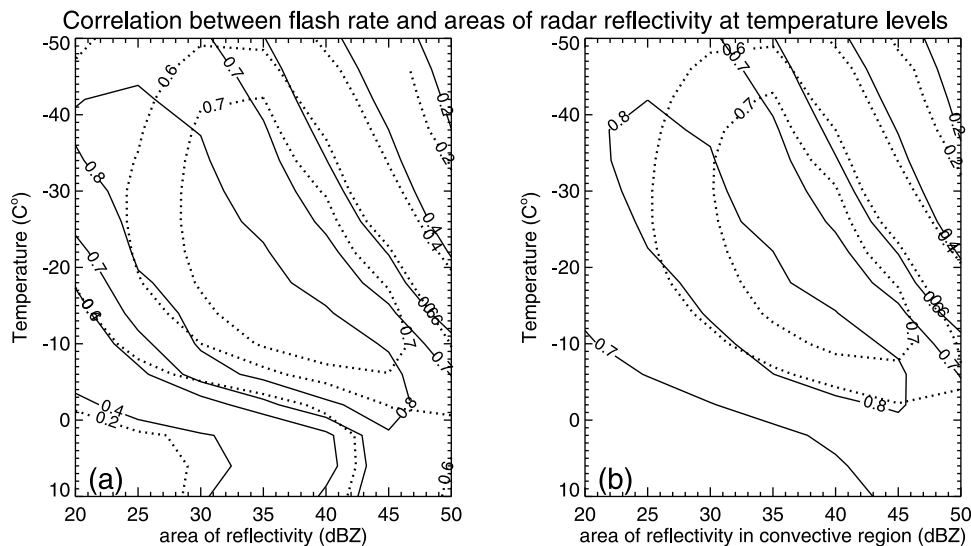
Figure 8. (a) Correlation coefficients between flash rates and the areas of radar reflectivity at different temperature levels in RPFs with flashes over land (solid) and ocean (dotted). (b) Same as Figure 8a but using only the convective portion of the RPFs defined by grouping the pixels with convective rainfall from TRMM PR 2A23. Note that the flash rate is calculated using flashes only inside the convective portion of the RPFs.
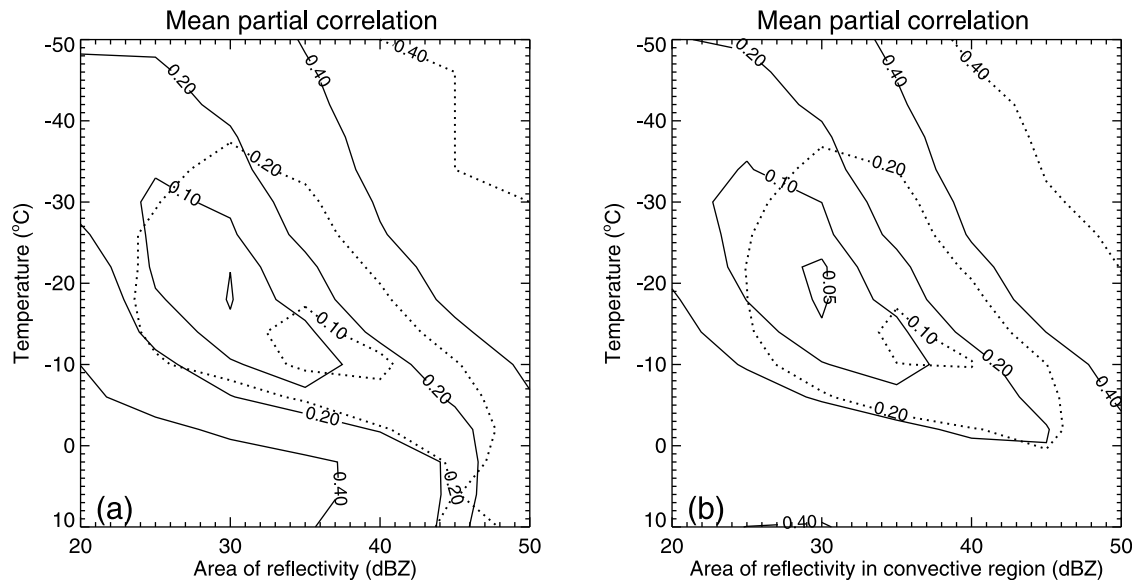
Figure 9. (a) Mean partial correlation coefficients between flash rates and the areas of radar reflectivity at different temperature levels in RPFs with flashes over land (solid) and ocean (dotted). The smaller value means that the area of the reflectivity at the temperature dominates the relationship to the flash rate. (b) Same as Figure 9a but using only the convective portion of the RPFs defined by grouping the pixels with convective rainfall from TRMM PR 2A23. Note that the flash rate is calculated using flashes only inside the convective portion of the RPFs.

possibly due to the inaccurate estimation of the reflectivity volumes with a coarse resolution of NCEP temperature profiles over high terrain.

[36] Having the same high correlation coefficients does not mean that the relationships between flash rate and these parameters of radar reflectivity are the same for different regions. Using a simple linear fitting equation:

$$\text{Flash rate} = A * \text{property of radar reflectivity} + B$$

The slope A and constant B are calculated to describe the best fit linear relationship between flash rate and properties of radar reflectivity in thunderstorms over land, ocean, and coastal region, as well as in each $4° \times 4°$ box. Note that with various storms under different weather regimes in the sample, the relationships between flash rate and the properties of the radar reflectivity are most likely nonlinear. Analysis here only demonstrates the relative variations of flash rates for given properties of radar reflectivity in general.

[37] The clearest differences are apparent between land and ocean, and these are summarized in Table 4. With few exceptions, the slope A is greater over land and coastal region than over ocean. With no exceptions, the slope A is greater for the 40 than the 35 dBZ measures and greater for the 35 than the 30 dBZ measures. In summary, other things being equal, the flash rate increases more rapidly with area or volume of reflectivity exceeding greater threshold values. The regional variations of these best fit parameters are mostly consistent with this generalization, although the constant B is not as consistent.

[38] Figure 11 shows that the slope A has some regional variations in relationships between flash rate and the area of 35 dBZ at $-10°C$ (Figure 11a), volume of 35 dBZ (Figure 11c), and IWC in volume of 30 dBZ (Figure 11e). In general, as the area or volume with high reflectivity increases, more additional flashes would be observed in thunderstorms over land than those over ocean. Some areas known for strong storms such as Amazon, Central Africa, Australia, Florida, and Southeast Asia have greater value of slope A than other land regions. Those are mostly in the tropics. Other areas known for strong storms in the subtropics such as southeastern South America, south central United States, and the Indian subcontinent have lesser values for the slope A. Bay of Bengal and ocean near Caribbean islands have higher slope A than most other oceans. It is interesting that high values of the constant B are found over south central United States, central Africa, Argentina, and Pakistan (Figures 11b, 11d, and 11f), also regions that have the strongest thunderstorms [*Zipser et al.*, 2006]. These regional variations indicate that the flash rate could be different in thunderstorms with similar radar properties over different regions. For example, for a large thunderstorm with 1000 km^2 area of 35 dBZ at $-10°C$, the average flash rate would be around 80 flash/min if it occurs over central Africa, around 40 flash/min if over the southwest United States, and could be as low as 5 flash/min over the open ocean.

[39] The variation in relationships between flash rate and IWC for land, ocean, and near-coastal regions seems larger than the findings of *Petersen et al.* [2005], especially with their conclusion that land and ocean relationships between flash density and integrated ice mass can be viewed as invariant on a global scale between land, ocean, and coastal regimes. Their TRMM radar-derived ice water path (IWP) had smaller differences in the relationships with flash rate density for land, ocean, and coastal regions than the results shown in this study (e.g., Table 4). But the sense of those differences, while smaller, is in agreement with our results that other things being equal, the flash rate increases with
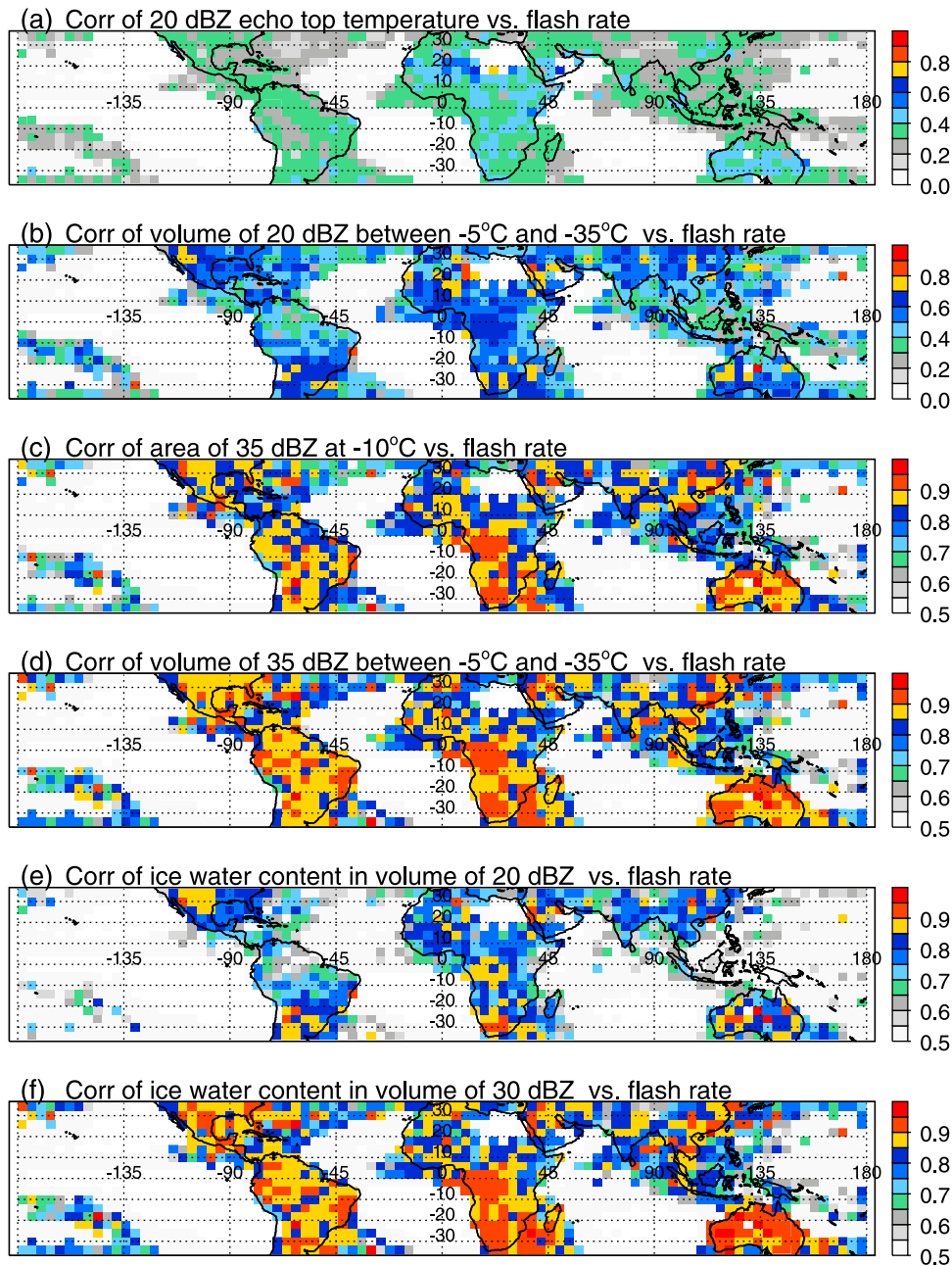
Figure 10. Correlation coefficients between flash rate and (a) 20 dBZ echo top temperature, (b) volume of 20 dBZ between −5°C and −35°C, (c) area of 35 dBZ at −10°C, (d) volume of 35 dBZ between −5°C and −35°C, (e) IWC in the volume of 20 dBZ from −5°C to echo top, and (f) IWC in the volume of 30 dBZ to echo top, in the RPFs with flash within 4° × 4° boxes. Note that the color scale in Figures 10a and 10b is different from Figures 10c–10f. The results are only shown for boxes with at least 20 samples.

estimated IWP faster over land than over ocean. In addition to the different sample size, the differences between the results here and *Petersen et al.* [2005] might be from the different methodologies. Petersen et al.'s "ensemble" approach comparing the IWP and flash rate density for coincidently observed 0.5° grid boxes that could include contributions from multiple small convective systems within the boxes, also could split the large MCSs into different boxes (see the spectrum of the thunder RPF size in Figure 5a). Their computation of IWP used a slightly different formula with a higher density of ice particles for high

reflectivity values (W. Petersen, personal communication, 2011). Their IWP included all PR measured reflectivities above the −10°C level but in convective cells only. Here the IWC are calculated for volumes with high values of reflectivities from −5°C to −35°C only from RPFs with lightning flashes. Perhaps the biggest difference is that Petersen et al.'s approach would have included the contribution to IWP from RPFs that had convection but no observed lightning. We note that the smallest land-ocean differences in our Table 4 are in area and volume of >40 dBZ echo, likely to be more closely related to IWP than some of the other parameters.

Table 4. Slope A and Constant B of Linear Fit Between Flash Rate and Area Exceeding Reflectivity Thresholds at −10°C and Volume Exceeding Reflectivity Thresholds and IWC in the Volume Exceeding 30 dBZ Over Land, Ocean, and Coastal Region

		Ocean		Land		Coast	
	Volume	Slope A (number/min/km^2)	Slope B (number/min/km^2)	Slope A (number/min/km^2)	Slope B (number/min)	Slope A (number/min/km^2)	Slope B (number/min)
Area at −10°C	30 dBZ	0.008	−0.10	0.026	−0.085	0.021	−0.83
	35 dBZ	0.025	0.14	0.052	0.78	0.050	0.051
	40 dBZ	0.075	0.92	0.11	2.27	0.12	1.63

		Ocean		Land		Coast	
	Volume	Slope A (number/min/km^2)	Slope B (number/min)	Slope A (number/min/km^3)	Slope B (number/min)	Slope A (number/min/km^3)	Slope B (number/min)
Volume between −5°C and −35°C	30 dBZ	0.004	−0.095	0.010	0.15	0.009	−0.81
	35 dBZ	0.013	0.132	0.020	1.33	0.022	0.41
	40 dBZ	0.040	0.890	0.043	2.88	0.052	1.99

		Ocean		Land		Coast	
	Volume	Slope A (number/min/km^6)	Slope B (number/min)	Slope A (number/min/km^6)	Slope B (number/min)	Slope A (number/min/km^6)	Slope B (number/min)
IWC between −5°C and −35°C	30 dBZ	0.009	−0.14	0.016	1.27	0.016	0.042

In addition to the IWP comparison, our Figure 11 and Table 4 do show substantial differences in some of the relationships between land and ocean, so it may be premature to conclude that differences are small without additional research.

4.4. Regional Variation of the Characteristics of the Radar Reflectivity in Thunderstorms

[40] To interpret the large spread of the samples in Figure 6 as well as the regional variations of the correlations from the properties of thunderstorms to the flash rate in the last section, it is important to understand the regional variations of the properties of thunderstorms. Median values of 20, 30, and 40 dBZ echo top temperatures in the RPFs with at least one flash are shown in 4° × 4° boxes in Figure 12. The thunderstorms in the tropics have colder 20 dBZ echo top temperatures than those in subtropics, and those over tropical oceans have relatively colder 20 dBZ echo top temperature than those over tropical land (Figure 12a). Median values of 30 and 40 dBZ echo top temperatures in RPFs with flashes over central Africa, Argentina, and southeast United States are colder than most of other regions (Figures 12b and 12c). This is consistent with the regions with the strongest thunderstorms [*Zipser et al.*, 2006]. In general, RPFs with flashes in the subtropics have colder median values of 40 dBZ echo top temperatures than those in the tropics, except central Africa (Figure 12c).

[41] To demonstrate the regional characteristics of thunderstorms with a "marginal" convective intensity for having lightning, the top 5% of the warmest 20, 30, and 40 dBZ echo top temperatures in RPFs with flashes are shown in 4° × 4° boxes in Figure 13. Note that the warm echo tops off the coast of Argentina are very likely due to false lightning detections caused by the South Atlantic Anomaly [*Boccippio et al.*, 2002], leading to more than 5% incorrect categorization of thunderstorms over the region. Consistent with it being "harder" to have a flash over ocean, the marginal 20 and 30 dBZ echo top temperatures for thunderstorms over ocean are colder than those over land (Figures 13a and 13b). For

example, the marginal 20 and 30 dBZ echo temperature for thunderstorms over tropical Pacific (10°S–10°N, 135°E–135°W) are about −21 and −5°C, comparing to −18.5 and −2°C for thunderstorms over Central Africa (10°S–10°N, 5°E–35°E). Over some desert and mountain regions, such as Sahel, Ethiopia, Iran, Tibet, Rocky Mountains, the "marginal" thunderstorms have colder 30 dBZ echo tops (Figure 13b). This is probably due to the fact that storms over these regions have high, cold cloud bases, so their echo tops are necessarily colder and higher even if cloud depth is not great.

[42] To compare the properties of thunderstorms over specific land and ocean regions, the frequency distribution of maximum PR reflectivity as a function of temperature is shown for thunderstorms over selected regions (Figure 14). Consistent with the earlier results in Figure 2, even the "bottom 10%" of thunderstorms over different regions have 30–35 dBZ in the mixed phase (−10° to −20°C) regions (Figure 14c). Also consistent with earlier results, the ocean regions have higher reflectivities for the marginal cases than the land regions (Figure 14c). Note that the low bottom 10% of reflectivity values below −10°C thunderstorms over the Indian and Pakistan (Figure 14c) are due to the samples over mountain regions. It is clear that most of thunderstorms over the tropical Atlantic, Pacific, and Indian Ocean have lower radar reflectivity in the mixed phase regions than those over land, except those over Amazon (Figure 14a). Over land, the Amazon region seems to be a special case. Even the strongest 10% of thunderstorms over Amazon are more like those over ocean (Figure 14b). This is consistent with the "green ocean" concept of the Amazon [*Silva Dias et al.*, 2002] that the convection in the region exhibits some of the properties of oceanic convection, especially in the rainy season when the air is known to be quite clean, with fewer aerosols. However, lightning flashes over Amazon are still more likely than over oceans (Figures 1b, 1e, 3, and 4). For a given volume of ice in the mixed phase region, thunderstorms over Amazon also have a higher flash rate than those over ocean (Figures 11a,
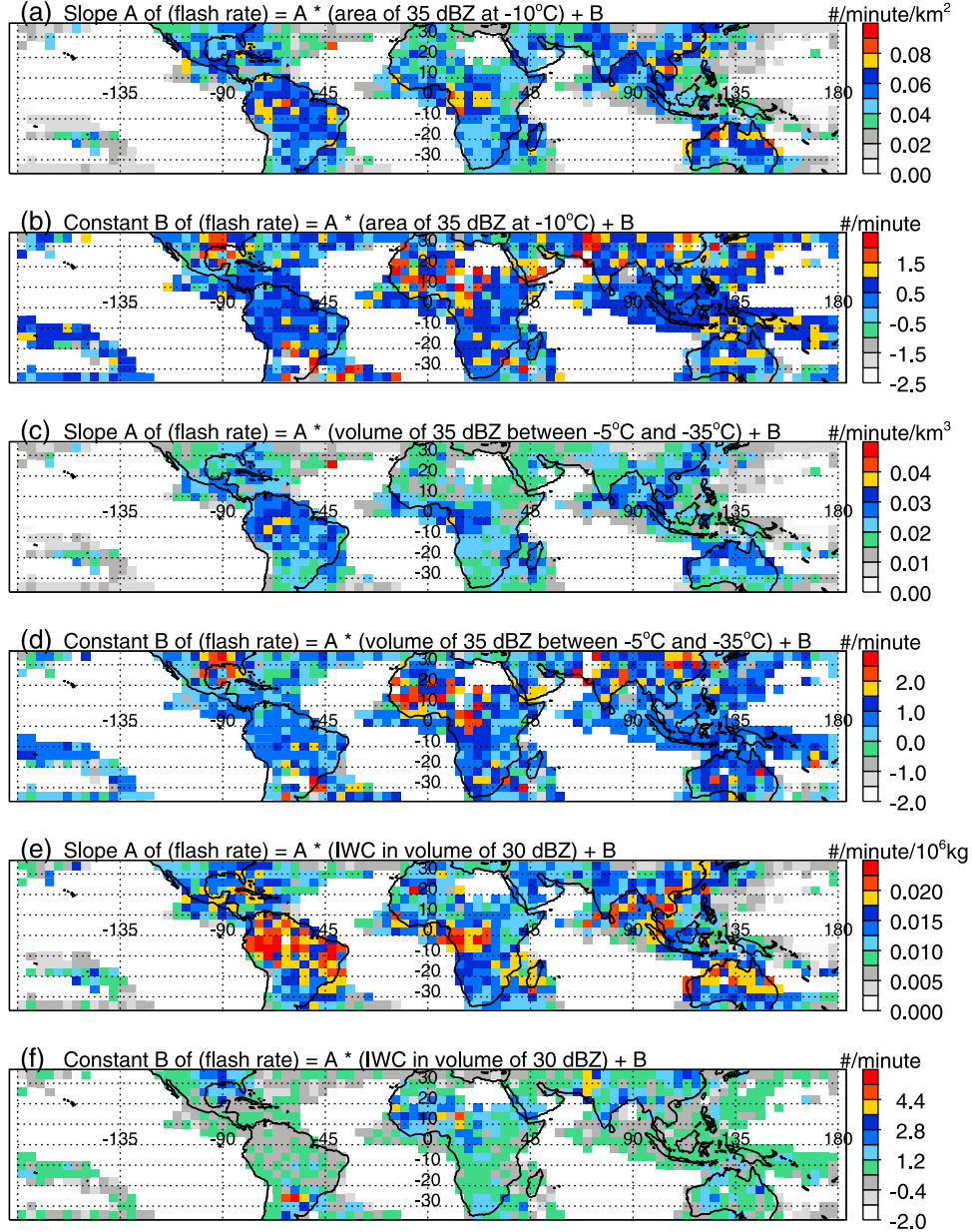
Figure 11. Parameters of linear fit between flash rate and selected properties in RPFs within $4° \times 4°$ boxes, including slope A and constant B of linear fit between flash rate and (a and b) area of 35 dBZ at $-10°C$, (c and d) volume of 35 dBZ between $-5°C$ and $-35°C$, and (e and f) ice water content in volume with 30 dBZ.
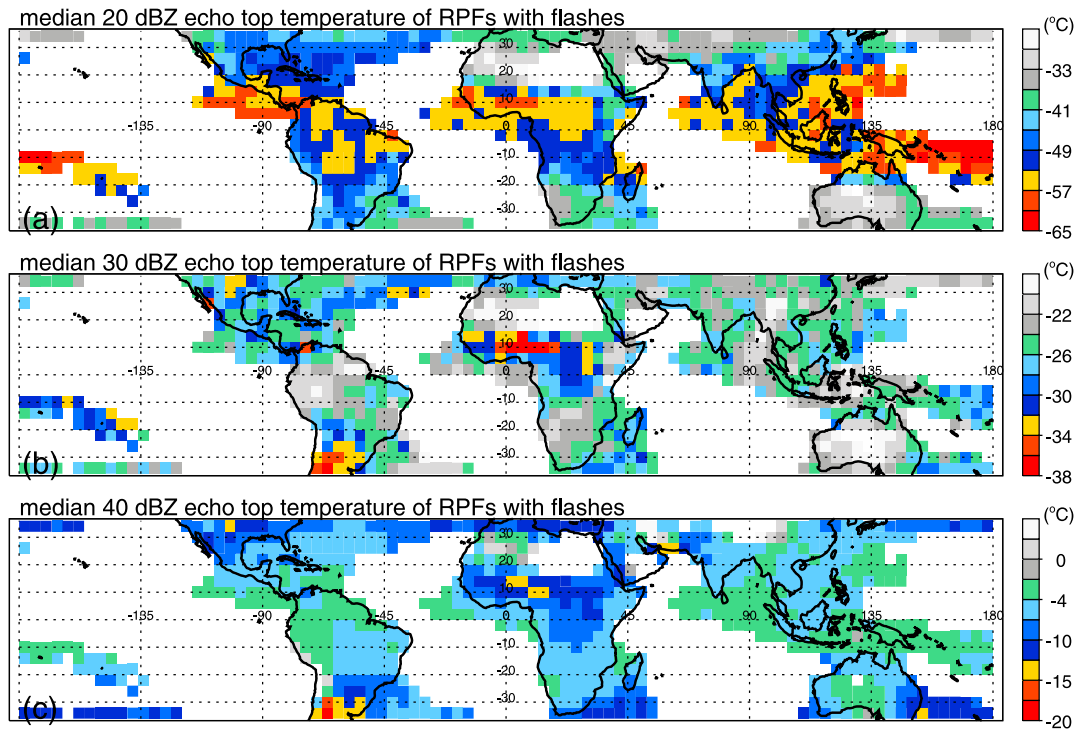
Figure 12. (a) Median values of 20 dBZ echo top temperatures of RPFs with flashes in 4° × 4° boxes during 1998–2010. (b) Same as Figure 12a, but for median values of 30 dBZ echo top temperatures. (c) Same as Figure 12a, but for median values of 40 dBZ echo top temperatures. Results only show for 4° × 4° boxes with at least 20 samples.
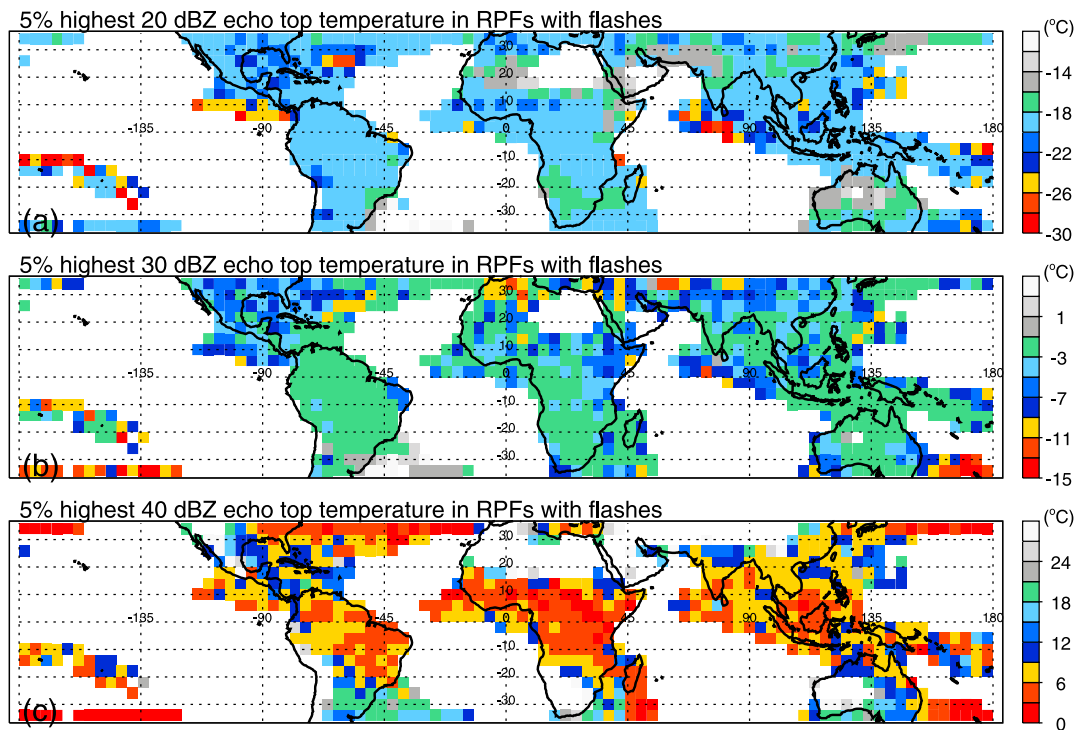
Figure 13. (a) Top 5% of the highest 20 dBZ echo top temperatures of RPFs with flashes in 4° × 4° boxes during 1998–2010. (b) Same as Figure 13a, but for top 5% of the highest 30 dBZ echo top temperatures. (c) Same as Figure 13a, but for top 5% of the highest 40 dBZ echo top temperatures. Results only show for 4° × 4° boxes with at least 20 samples.
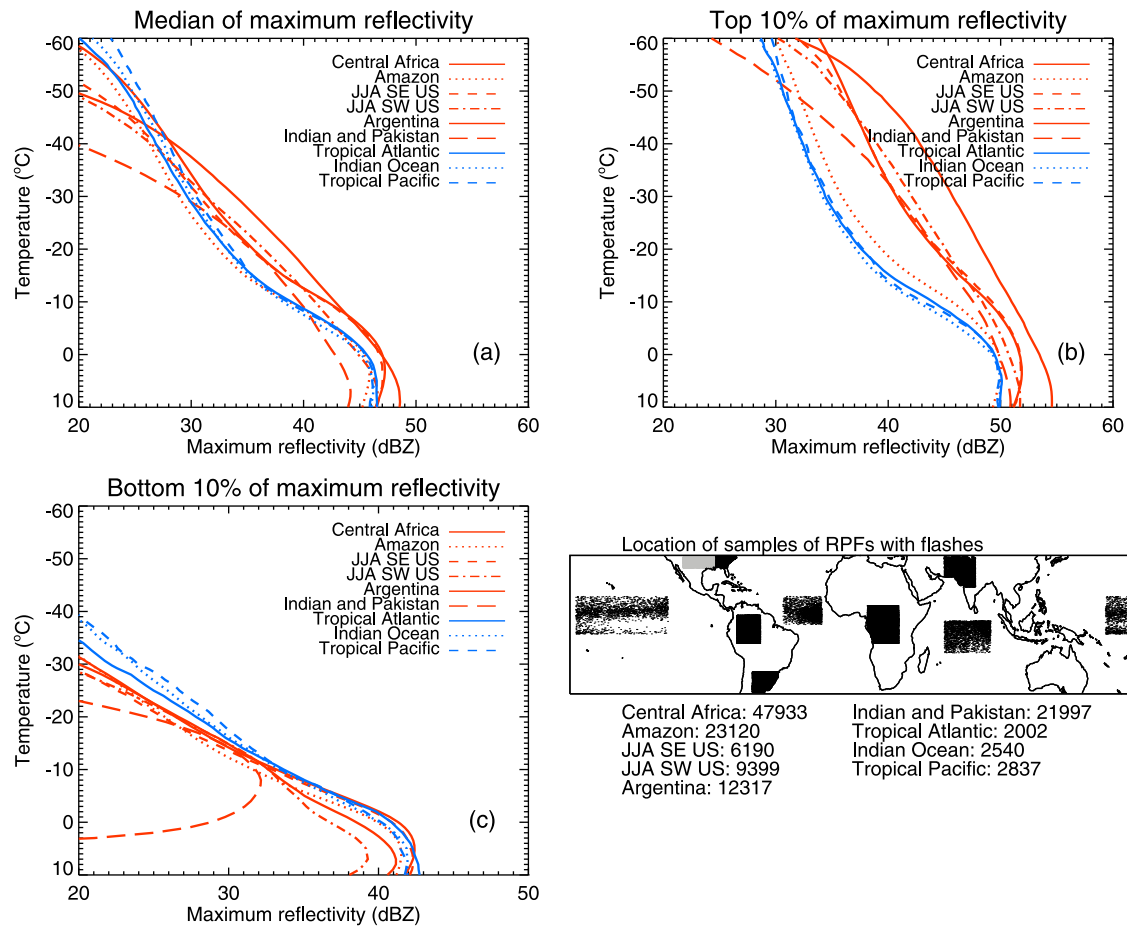
Figure 14. Frequency distribution of maximum PR reflectivity at temperature levels in thunderstorms over different regions. (a) Median of maximum reflectivity at temperature levels, (b) top 10% of maximum reflectivity, and (c) bottom 10% of maximum reflectivity. On the bottom right are locations and numbers of the samples.

11c, and 11e). This is currently still a mystery that requires further investigation.

5. Conclusions

[43] Using 13 years of TRMM PR and LIS observations, the relationships between lightning flash rate and radar reflectivity structures are investigated over the global tropics and subtropics. Some of the results confirm the conclusions of existing studies, such as the following:

[44] 1. There are more lightning flashes over land than over ocean. With the same radar reflectivity properties, lightning flashes over land are more probable than over ocean. Flashes are more probable over oceans within about 1000 km downwind of landmasses than over the open oceans but not as probable as over land.

[45] 2. There is a high correlation between flash rate and the volume of high radar reflectivity in the mixed phase region. The flash rate is better correlated with the area and volume of high radar reflectivity in the mixed phase region (e.g., >35 dBZ between $-5°$ to $-35°C$) than with the proxies of maximum convective intensity of the thunderstorms.

[46] 3. Correlations between flash rate and the area satisfying radar reflectivity thresholds at different temperature levels reaffirm the importance of the presence of large ice particles with high radar reflectivity in the charging zone.

[47] Some results are presented with a large sample for the first time.

[48] 1. While the existence of 30 dBZ at $-40°C$ or 40 dBZ at $-12°C$ is a very good indicator of the probability of lightning, regional variations are also found in addition to the expected land versus ocean contrast. The probability of lightning is greater for the Amazon than for subtropical South America and greater for subtropical oceans than near-equatorial oceans, for reflectivity-temperature thresholds that were examined.

[49] 2. With a large sample, it is statistically and quantitatively shown that area of echo exceeding 30–40 dBZ between $-10°C$ to $-20°C$ is more important in the correlations to the flash rate than the area exceeding 20 dBZ at any temperature. This is still more direct evidence of the dominance of the noninductive charging process in the thunderstorms. The best correlations over ocean tend to be for somewhat higher dBZ values and somewhat colder echo tops than those over land.

[50] 3. There are regional variations of the relationships between the flash rate and the volume of the high radar reflectivity in the mixed phase region, in addition to the typical land versus ocean contrast. A given volume of

35+ dBZ echo in the mixed phase region would predict a greater flash rate in tropical Africa or tropical South America than in the subtropics and would predict a far lower flash rate over the oceans. This is consistent with the large regional variations of relationships between the flash rates and the areas of cold microwave brightness temperatures in thunderstorms [*Liu et al.*, 2011].

[51] To understand these regional variations, probably we will have to look into the relation of lightning flashes and the radar reflectivity in different kinds of weather regimes in different seasons. Thunderstorms of different weather regimes and aerosol environments are very likely to have different microphysical processes affecting the size distributions of precipitation ice particles and supercooled liquid water contents. The detailed analysis of the flash rates in the storms with similar radar reflectivity vertical structures will be useful in understanding these physical processes in the future. The optical lightning detectors planned for upcoming geostationary satellites from the United States, Europe, and China also hold great promise for this line of research. For places with research quality radar networks in the field of view of those sensors, time lags between radar signatures and lightning flash rate can be investigated.

References

Atlas, D. (1958), Radar lightning echoes and atmospherics in vertical cross section, in *Recent Advances in Atmospheric Electricity*, edited by L. G. Smith, pp. 441–459, Pergamon, New York.

Awaka, J., T. Iguchi, and K. Okamoto (1998), Early results on rain type classification by the Tropical Rainfall Measuring Mission (TRMM) precipitation radar, paper presented at 8th Commission F Open Symposium, Int. Union of Radio Sci., Aveiro, Portugal.

Boccippio, D. K., S. J. Goodman, and S. Heckman (2000), Regional differences in tropical lightning distributions, *J. Appl. Meteorol.*, *39*, 2231–2248, doi:10.1175/1520-0450(2001)040<2231:RDITLD>2.0.CO;2.

Boccippio, D. J., W. J. Koshak, and R. J. Blakeslee (2002), Performance assessment of the Optical Transient Detector and Lightning Imaging Sensor. Part I: Predicted diurnal variability, *J. Ocean Technol.*, *19*, 1318–1332, doi:10.1175/1520-0426(2002)019<1318:PAOTOT>2.0.CO;2.

Carey, L. D., and S. T. Rutledge (2000), The relationship between precipitation and lightning in tropical island convection: A C-bandpolarimetric radar study, *Mon. Weather Rev.*, *128*, 2687–2710, doi:10.1175/1520-0493(2000)128<2687:TRBPAL>2.0.CO;2.

Cecil, D. J., and E. J. Zipser (2002), Reflectivity, ice scattering, and lightning characteristics of hurricane eyewalls and rainbands. Part II: Intercomparison of observations, *Mon. Weather Rev.*, *130*, 769–784, doi:10.1175/1520-0493(2002)130<0769:RISALC>2.0.CO;2.

Cecil, D. J., S. J. Goodman, D. J. Boccippio, E. J. Zipser, and S. W. Nesbitt (2005), Three years of TRMM precipitation features. Part I: Radar, radiometric, and lightning characteristics, *Mon. Weather Rev.*, *133*, 543–566, doi:10.1175/MWR-2876.1.

Christian, H. J., et al. (2003), Global frequency of lightning as observed from space by the optical transient detector, *J. Geophys. Res.*, *108*(D1), 4005, doi:10.1029/2002JD002347.

Deierling, W., and W. A. Petersen (2008), Total lightning activity as an indicator of updraft characteristics, *J. Geophys. Res.*, *113*, D16210, doi:10.1029/2007JD009598.

Deierling, W., W. A. Petersen, J. Latham, S. Ellis, and H. J. Christian (2008), The relationship between lightning activity and ice fluxes in thunderstorms, *J. Geophys. Res.*, *113*, D15210, doi:10.1029/2007JD009700.

Fierro, A. O., M. S. Gilmore, E. R. Mansell, L. J. Wicker, and J. M. Straka (2006), Electrification and lightning in an idealized boundary-crossing supercell simulation of 2 June 1995, *Mon. Weather Rev.*, *134*, 3149–3172, doi:10.1175/MWR3231.1.

Goodman, S. J., and H. J. Christian Jr. (1993), Global observations of lightning, in *Atlas of Satellite Observations Related to Global Change*, edited by R. J. Gurney et al., pp. 191–219, Cambridge Univ. Press, Cambridge, U. K.

Iguchi, T., T. Kozu, R. Meneghini, J. Awaka, and K. Okamoto (2000), Rain-profiling algorithm for the TRMM precipitation radar, *J. Appl. Meteorol.*, *39*, 2038–2052, doi:10.1175/1520-0450(2001)040<2038:RPAFTT>2.0.CO;2.

Kistler, R., et al. (2001), The NCEP-NCAR 5—Year reanalysis: Monthly means CD-ROM and documentation, *Bull. Am. Meteorol. Soc.*, *82*, 247–267, doi:10.1175/1520-0477(2001)082<0247:TNNYRM>2.3.CO;2.

Kummerow, C., W. Barnes, T. Kozu, J. Shiue, and J. Simpson (1998), The Tropical Rainfall Measuring Mission (TRMM) sensor package, *J. Atmos. Oceanic Technol.*, *15*, 809–817, doi:10.1175/1520-0426(1998)015<0809:TTRMMT>2.0.CO;2.

Lang, T. J., S. A. Rutledge, J. E. Dye, M. Venticinque, P. Laroche, and E. Defer (2000), Anomalously low negative cloud-to-ground lightning flash rates in intense convective storms observed during STERAO-A, *Mon. Weather Rev.*, *128*, 160–173, doi:10.1175/1520-0493(2000)128<0160:ALNCTG>2.0.CO;2.

Liu, C., E. Zipser, and S. W. Nesbitt (2007), Global distribution of tropical deep convection: Different perspectives using infrared and radar as the primary data source, *J. Clim.*, *20*, 489–503, doi:10.1175/JCLI4023.1.

Liu, C., E. J. Zipser, D. J. Cecil, S. W. Nesbitt, and S. Sherwood (2008), A cloud and precipitation feature database from 9 years of TRMM observations, *J. Appl. Meteorol. Climatol.*, *47*, 2712–2728, doi:10.1175/2008JAMC1890.1.

Liu, C., E. R. Williams, E. J. Zipser, and G. Burns (2010), Diurnal variations of global thunderstorms and electrified shower clouds and their contribution to the global electrical circuit, *J. Atmos. Sci.*, *67*, 309–323, doi:10.1175/2009JAS3248.1.

Liu, C., D. J. Cecil, and E. J. Zipser (2011), Relationships between lightning flash rates and passive microwave brightness temperatures at 85 and 37 GHz over the tropics and subtropics, *J. Geophys. Res.*, *116*, D23108, doi:10.1029/2011JD016463.

Lucas, C., E. Zipser, and M. LeMone (1994), Vertical velocity in oceanic convection off tropical Australia, *J. Atmos. Sci.*, *51*, 3183–3193, doi:10.1175/1520-0469(1994)051<3183:VVIOCO>2.0.CO;2.

MacGorman, D. R., and W. D. Rust (1999), *The Electrical Nature of Storms*, 422 pp., Oxford Univ. Press, New York.

Marshall, J. S., and S. Radhakant (1978), Radar precipitation maps as lightning indicators, *J. Appl. Meteorol.*, *17*, 206–212, doi:10.1175/1520-0450(1978)017<0206:RPMALI>2.0.CO;2.

Mosier, R. M., C. Schumacher, R. E. Orville, and L. D. Carey (2011), Radar nowcasting of cloud-to-ground lightning over Houston, Texas, *Weather Forecast.*, *26*, 199–212, doi:10.1175/2010WAF2222431.1.

Orville, R. E., and R. W. Henderson (1986), Global distribution of midnight lightning: September 1977 to August 1978, *Mon. Weather Rev.*, *114*, 2640–2653, doi:10.1175/1520-0493(1986)114<2640:GDOMLS>2.0.CO;2.

Pessi, A. T., and S. Businger (2009), Relationships among lightning, precipitation, and hydrometeor characteristics over the North Pacific Ocean, *J. Appl. Meteorol. Climatol.*, *48*, 833–848, doi:10.1175/2008JAMC1817.1.

Petersen, W. A., and S. A. Rutledge (2001), Regional variability in tropical convection: Observations from TRMM, *J. Clim.*, *14*, 3566–3586, doi:10.1175/1520-0442(2001)014<3566:RVITCO>2.0.CO;2.

Petersen, W. A., S. A. Rutledge, and R. W. Orbille (1996), Cloud-to-ground lightning observations from TOGA COARE: Selected results and lightning location algorithms, *Mon. Weather Rev.*, *124*, 602–620, doi:10.1175/1520-0493(1996)124<0602:CTGLOF>2.0.CO;2.

Petersen, W. A., H. J. Christian, and S. A. Rutledge (2005), TRMM observations of the global relationship between ice water content and lightning, *Geophys. Res. Lett.*, *32*, L14819, doi:10.1029/2005GL023236.

Rutledge, S. A., and W. A. Petersen (1994), Vertical radar reflectivity structure and cloud-to-ground lightning in the stratiform region of MCSs: Further evidence for in situ charging in the stratiform region, *Mon. Weather Rev.*, *122*, 1760–1776, doi:10.1175/1520-0493(1994)122<1760:VRRSAC>2.0.CO;2.

Rutledge, S. A., C. Lu, and D. R. MacGorman (1990), Positive cloud-to-ground lightning in mesoscale convective systems, *J. Atmos. Sci.*, *47*, 2085–2100, doi:10.1175/1520-0469(1990)047<2085:PCTGLI>2.0.CO;2.

Saunders, C. P. R., and S. L. Peck (1998), Laboratory studies of the influence of the rime accretion rate on charge transfer during crystal/graupel collisions, *J. Geophys. Res.*, *103*, 13,949–13,956, doi:10.1029/97JD02644.

Shackford, C. R. (1960), Radar indications of a precipitation-lightning relationship in New England thunderstorms, *J. Meteorol.*, *17*, 15–19, doi:10.1175/1520-0469(1960)017<0015:RIOAPL>2.0.CO;2.

Silva Dias, M. A. F., et al. (2002), Cloud and rain processes in a biosphere-atmosphere interaction context in the Amazon region, *J. Geophys. Res.*, *107*(D20), 8072, doi:10.1029/2001JD000335.

Stith, J. L., J. A. Haggerty, A. Heymsfield, and C. A. Grainger (2004), Microphysical characteristics of tropical updrafts in clean conditions, *J. Appl. Meteorol.*, *43*, 779–794, doi:10.1175/2104.1.

Takahashi, T. (1978), Riming electrification as a charge generation mechanism in thunderstorms, *J. Atmos. Sci.*, *35*, 1536–1548, doi:10.1175/1520-0469(1978)035<1536:REAACG>2.0.CO;2.

Toracinta, E. R., D. J. Cecil, E. J. Zipser, and S. W. Nesbitt (2002), Radar, passive microwave and lightning characteristics of precipitating systems in the tropics, *Mon. Weather Rev.*, *130*, 802–824, doi:10.1175/1520-0493(2002)130<0802:RPMALC>2.0.CO;2.

Ushio, T., S. J. Heckman, D. J. Boccippio, H. J. Christian, and Z.-I. Kawasaki (2001), A survey of thunderstorm flash rates compared to cloud top height using TRMM satellite data, *J. Geophys. Res.*, *106*, 24,089–24,095, doi:10.1029/2001JD900233.

Vincent, B. R., L. D. Carey, D. Schneider, K. Keeter, and R. Gonski (2003), Using WSR-88D reflectivity for the prediction of cloud-to-ground lightning: A central North Carolina study, *Natl. Weather Digest*, *27*, 35–44.

Vorpahl, J. A., J. G. Sparrow, and E. P. Ney (1970), Satellite observations of lightning, *Science*, *169*, 860–862, doi:10.1126/science.169.3948.860.

Wang, C. P. (1963), Lightning discharges in the tropics: 1. Whole discharges, *J. Geophys. Res.*, *68*, 1943–1949, doi:10.1029/JZ068i007p01943.

Wiens, K. C., S. A. Rutledge, and S. A. Tessendorf (2005), The 29 June 2000 supercell observed during STEPS. Part II: Lightning and charge structure, *J. Atmos. Sci.*, *62*, 4151–4177, doi:10.1175/JAS3615.1.

Williams, E. R. (1985), Large-scale charge separation in thunderclouds, *J. Geophys. Res.*, *90*, 6013–6025, doi:10.1029/JD090iD04p06013.

Williams, E. R., and S. G. Geotis (1989), A radar study of the plasma and geometry of lightning, *J. Atmos. Sci.*, *46*, 1173–1185, doi:10.1175/1520-0469(1989)046<1173:ARSOTP>2.0.CO;2.

Williams, E. R., and S. B. Stanfill (2002), The physical origin of the land-ocean contrast in lightning activity, *C. R. Phys.*, *3*, 1277–1292, doi:10.1016/S1631-0705(02)01407-X.

Williams, E. R., M. E. Weber, and R. E. Orville (1989), The relationship between lightning type and convective state of thunderclouds, *J. Geophys. Res.*, *94*, 13,213–13,220, doi:10.1029/JD094iD11p13213.

Workman, E. J., and S. E. Reynolds (1949), Electrical activity as related to thunderstorm cell growth, *Bull. Am. Meteorol. Soc.*, *30*, 142–144.

Xu, W., E. J. Zipser, C. Liu, and J. Jiang (2010), On the relationships between lightning frequency and thundercloud parameters of regional precipitation systems, *J. Geophys. Res.*, *115*, D12203, doi:10.1029/2009JD013385.

Zipser, E. J., and K. R. Lutz (1994), The vertical profile of radar reflectivity of convective cells: A strong indicator of storm intensity and lightning probability?, *Mon. Weather Rev.*, *122*, 1751–1759, doi:10.1175/1520-0493(1994)122<1751:TVPORR>2.0.CO;2.

Zipser, E. J., D. Cecil, C. Liu, S. Nesbitt, and D. Yorty (2006), Where are the most intense thunder storms on Earth?, *Bull. Am. Meteorol. Soc.*, *87*, 1057–1071, doi:10.1175/BAMS-87-8-1057.

D. J. Cecil, Earth System Science Center, University of Alabama in Huntsville, Huntsville, AL 35899, USA.

K. Kronfeld and R. Robertson, Rockwell Collins, 400 Collins Rd. NE, Cedar Rapids, IA 52498, USA.

C. Liu and E. J. Zipser, Department of Atmospheric Sciences, University of Utah, Salt Lake City, UT 84112, USA. (liu.c.t@utah.edu)